Received: 14 July 2017 | Revised: 6 March 2018 | Accepted: 16 March 2018
DOI: 10.1002/pip.3034

EU PVSEC PAPER

WILEY PROGRESS IN PHOTOVOLTAICS

Wafer integrated micro-scale concentrating photovoltaics

Duanhui Li[1†] | Lan Li[1†] | Bradley Jared[2] | Gordon Keeler[2] | Bill Miller[2] | Michael Wood[2] | Christopher Hains[2] | William Sweatt[2] | Scott Paap[2] | Michael Saavedra[2] | Charles Alford[2] | John Mudrick[2] | Ujjwal Das[3] | Steve Hegedus[3] | Anna Tauke-Pedretti[2] | Juejun Hu[1] | Tian Gu[1]

[1] Massachusetts Institute for Technology, Cambridge, MA, USA

[2] Sandia National Laboratories, Albuquerque, NM, USA

[3] Institute of Energy Conversion, University of Delaware, Newark, DE, USA

Correspondence
Anna Tauke-Pedretti, Sandia National Laboratories, Albuquerque, NM, USA.
Email: ataukep@sandia.gov

Juejun Hu and Tian Gu, Massachusetts Institute for Technology, Cambridge, MA, USA.
Email: hujuejun@mit.edu; gutian@mit.edu

Funding information
Advanced Research Projects Agency - Energy, Grant/Award Number: DE-AR0000632

Abstract

A novel micro-scale photovoltaic concept, Wafer Integrated Micro-scale Photovoltaics (WPV), is proposed, analyzed, and experimentally demonstrated. The WPV concept seamlessly integrates multijunction micro-cells with a multi-functional silicon platform that simultaneously provides optical concentration, hybrid PV/CPV architecture, and mechanical alignment features. Fabrication and optical performance characterization of the Si platform are described in this paper. Over 100% improvement in the concentration-acceptance-angle product (*CAP*) is demonstrated using the wafer-embedded micro-concentrating elements, leading to significantly reduced module material and fabrication costs, sufficient angular tolerance for low-cost trackers, and an ultra-compact optical architecture compatible with commercial flat panel infrastructures. The development of a prototypical module with a 400× concentration ratio is described. Outdoor optical characterization of the module shows acceptance angles of ±1.7° and ±2.5° for 90% of on-axis power and full-width-half-maximum, respectively. The projected performance of the PV/CPV hybrid architecture illustrates its potential for cost-effective collection of both direct and diffuse sunlight, thereby extending the geographic and market domains for cost-effective PV system deployment. Leveraging low-cost micro-fabrication and high-level integration techniques, the WPV approach presents a promising route to combine the high performance of multijunction solar cells and the low costs of flat-plate Si PV systems.

KEYWORDS

c-Si, concentrators, multijunction solar cell, solar radiation

1 | INTRODUCTION

Solar energy production has witnessed dramatic growth in recent years taking advantage of the rapid price reduction of Si-wafer based photovoltaics (PV), driven by scaling-up of PV deployment volume and technological advancement.[1] However, as the efficiency of Si PV reaches its practical limit, balance-of-system (BOS) costs gradually becomes the dominant challenge for continued price reduction which saturates the cost learning curve.[2] High-efficiency, low-cost PV modules beyond Si are therefore critical for further market penetration and can potentially enable a new price learning curve for solar energy technology.

By utilizing high performance multijunction cells and concentrator optics, concentrating photovoltaics (CPV) systems can in principle reduce energy production costs by considerably reducing the usage of costly multijunction cells.[3-7] In recent years, the performance of CPV technologies has been advancing steadily, with cell and module conversion efficiencies reaching 46% and 43.4%, respectively.[8,9]

†These authors contributed equally to this work.

However, conventional CPV approaches are severely plagued by several issues that offset the potential cost effectiveness. At the module level, trade-offs exist among the cell, optics, and module manufacturing costs. At the system level, trade-offs exist between the module performance and system installation/operation costs.[10,11] In order to improve the concentration ratio and reduce multijunction cell area, complexity of the optical concentrator system has to be increased, which inevitably increases module fabrication costs. Using conventional concentrator optics, such need further poses stringent requirements on tracker accuracy, mandating dedicated CPV trackers incompatible with low-cost trackers designed for Si flat-panel PV. Moreover, the inability of conventional CPV to collect diffuse light further limits its geographic deployment and market penetration. Diffuse radiation component of the sunlight (ie, light scattered by atmospheric aerosols and clouds) constitutes a considerable portion of the total incident power that usually cannot be captured by conventional CPV systems due to the relatively small acceptance angle. Standard solar radiation data across the USA suggests that the contribution from diffuse radiation is approximately 2 to 2.5 kWh/m^2-day for all the locations studied, and the diffuse component represents 20% to 40% of the global radiation depending on the geographic location.[12]

The previously mentioned module-level and system-level cost issues associated with CPV are fundamentally imposed by the thermodynamic limit of optical concentrators which manifests as a trade-off between concentration ratio (C_g) and acceptance angle (θ_{in}), or, the conservation of étendue.[13,14] A key figure of merit for evaluating CPV systems is the concentration-acceptance product (CAP),

$$CAP = \sqrt{C_g}\sin\theta_{in} \tag{1}$$

Note that for a given optical architecture, *CAP* is nearly an invariant for different concentration ratios but can be improved by using advanced optical designs, eg, Miñano et al,[15] Gleckman et al,[16] and Welford and Winston.[17] Hence, Equation (1) reveals the trade-off between concentration ratio and acceptance angles and accordingly the balance among materials, module, and system level costs. With limited *CAP* values close to or below 0.5, state-of-the-art CPV technologies are typically designed for high concentrations to reduce cell costs, at the expenses of complex module designs and tight tolerances to assembly and operation misalignments.[3] For instance, CPV systems with concentration above 1000× necessitate high-precision module assembly and high-accuracy trackers (<1°), leading to significantly increased module fabrication and BOS costs that offset the performance and cost improvements at the cell level.

By dramatically scaling down the dimensions of multijunction cells to the 100's of microns regime and accordingly the concentrating optics (eg, ~ a few millimeters in diameter), micro-scale PV integrate arrays of micro-cells and micro-optics within a compact module similar to flat plate Si PV using advanced cell fabrication and massive parallel assembly approaches compatible with large-scale manufacturing.[10,18-29] Integrated hybrid micro-PV/CPV architectures can be utilized to combine high-performance micro-cells and low-cost flat plate PV, which would considerably improve overall power conversion efficiency.[21,24] Furthermore, embedded planar micro-tracking CPV using micro-cells is shown to be capable of significantly improving the energy output, particularly promising for rooftop and space-constrained implementations.[30] Potential benefits of exploiting micro-scale solar cells include enhanced cell performance, reduced semiconductor and optic materials costs, interconnect flexibility, improved heat dissipation, and a compact physical profile that facilitates installation and operation. Arrays of concentrators can be fabricated in the form of large area optical sheets via low-cost plastic molding.

It should be noted that simply miniaturizing traditional CPV modules based on fabrication and module assembly techniques optimized for macro-CPV is not a viable route to fulfilling the potential benefits of micro-scale PV due to their limited scalability. The reduction of component size further limits the employment of efficient non-imaging or multi-stage optical concentrator systems that could bring performance close to the thermodynamic limit, because the fabrication and assembly of such components in either micro-scale or large array is challenging and cost-prohibitive.

Here we argue that, in order to reach or even surpass the cost learning curve of Si PV technology, the following performance attributes are demanded for future concentrator-based PV: (1) high performance multijunction micro-cell arrays, (2) high efficiency, high concentration, and large field-of-view micro-optics that further reduce usage of semiconductor materials, simplify module design, and are tolerant to pointing accuracies of low-cost trackers (1°~1.5°tracking accuracy), (3) high level integration of the components within a compact module to minimize assembly and operation costs, (4) the module fabrication and BOS should be compatible with current Si PV manufacturing in order to take advantages of the economy of scale, and (5) diffuse light should be captured in a cost-effective manner.

In this paper, recent development of a new micro-scale PV concept is presented, aiming to radically improve PV system's cost effectiveness by further exploiting cell/optics scaling. The Wafer Integrated Micro-scale Photovoltaic (WPV) concept[10] utilizes III-V micro-cells integrated with a novel multifunctional Si platform to fully leverage the high performance of multijunction cells as well as module-level and system-level benefits of Si flat-plate PV. The PV system designs are guided by a detailed cost model based on industrial-scale fabrication processes that analyzes and predicts energy production costs.[31]

Here, we report the design, fabrication, integration, and optical performance characterization of the Si platform, which shows remarkable versatility for integration with different micro-cell and micro-optic architectures and significant improvement compared with conventional concentrator PV approaches. The development of a first baseline prototypical module is also described. In Section 2, the basic WPV concept and rationale is described and a baseline structure with a single primary lens is introduced. In Section 3, details of the fabrication process and characterization results of the Si platform are given. This is followed by the optical performance characterization of the etched Si cavity in Section 4. In Section 5, the development of the prototypical baseline module is described and initial optical performance characterization is discussed. Section 6 discusses the projected performance of the proposed approach under a variety of irradiation conditions.

2 | WAFER-INTEGRATED MICRO-SCALE PV/CPV: CONCEPT

As schematically illustrated in Figure 1, the key notion of the WPV concept is a multi-functional silicon platform integrating high concentration multijunction micro-cell arrays, cell interconnects, and high performance micro-optical elements all embedded at the wafer level. The Si cell contains etched truncated pyramid-shaped reflective cavities that serve as efficient non-imaging micro-optical concentrators and alignment features for other micro-optical/mechanical components (Figure 1B to D). The III-V cell is located at the bottom of the cavity, which provides concentration and increases the field of view of the entire optical system. It also improves the tolerance to fabrication errors and refractive index changes resulting from temperature variations. Anisotropic etching of standard {100} oriented silicon substrates exposes the {111} crystal planes to form truncated-pyramid-shaped rectangular cavities with facets of an 35.3° slanting angle. The 4 sidewall facets of the cavity are coated with highly reflective metal films. Optical apertures of the cavities are precisely defined to match the micro-scale cells. The Si cell is also designed to capture and convert the diffuse and off-alignment sunlight which usually contribute to major optical losses in conventional CPV systems. As a result, the WPV approach seamlessly integrates multiple functionalities on an ultra-compact hybrid IIIV-on-Si platform, including optical micro-concentration, hybrid PV/CPV photovoltaic, and mechanical micro-assembly.

As depicted in Figure 1B,C, a baseline WPV structure consists of (1) a 1X or low-concentration Si cell platform encompassing the reflective cavity arrays and cell interconnects, (2) a high-concentration multijunction micro-scale PV cell array integrated on the Si platform and aligned to the cavities, and (3) a primary concentrating optic array. Enabled by such wafer-level integrated micro-concentrators, the simple baseline WPV architecture yields prototype designs with concentration ratios ranging between 400× and 2400× while maintaining sufficient angular tolerances (±1°~ ±2°) that are fully compatible with commercial low-cost trackers designed for Si PV (typically 1°~1.5° tracking accuracy). Compared with high-precision trackers dedicated to traditional CPV modules, Si trackers have less demanding accuracy requirements, and their manufacturing can take advantage of the economy of scale to achieve considerably reduced costs. The Si platform with the cavities as on-wafer alignment features can be further integrated with a variety of single-stage or multi-stage optical concentrator architectures while maintaining a compact form factor. Analyses and experimental investigations described in later sections suggest the WPV approach can potentially leverage both the high performance of multijunction cells and the low cost of flat plate Si PV infrastructures at the module- and system-levels.

3 | Si PLATFORM FABRICATION AND CHARACTERIZATION

The fabrication process for the multifunctional Si platform is schematically illustrated in Figure 2. The process starts with standard PV-grade double-side polished Si wafers with 280-μm thickness. The truncated-pyramid cavities were defined via anisotropic wet etching in an aqueous solution containing 36% KOH and 10% isopropanol (by weight) at 90°C. Silicon nitride (400-nm thickness) deposited by plasma enhanced chemical vapor deposition was used as the etch mask. The specific etching condition is optimized for generating smooth cavity sidewalls to minimize optical scattering loss. The nitride mask was stripped in 7:1 buffer oxide etch (BOE) after the etching step, and the wafer was subsequently encapsulated in a sputtered silicon nitride layer to prevent electrical shorting. Ti/Au interconnects, Ti/Au/Ni/Au

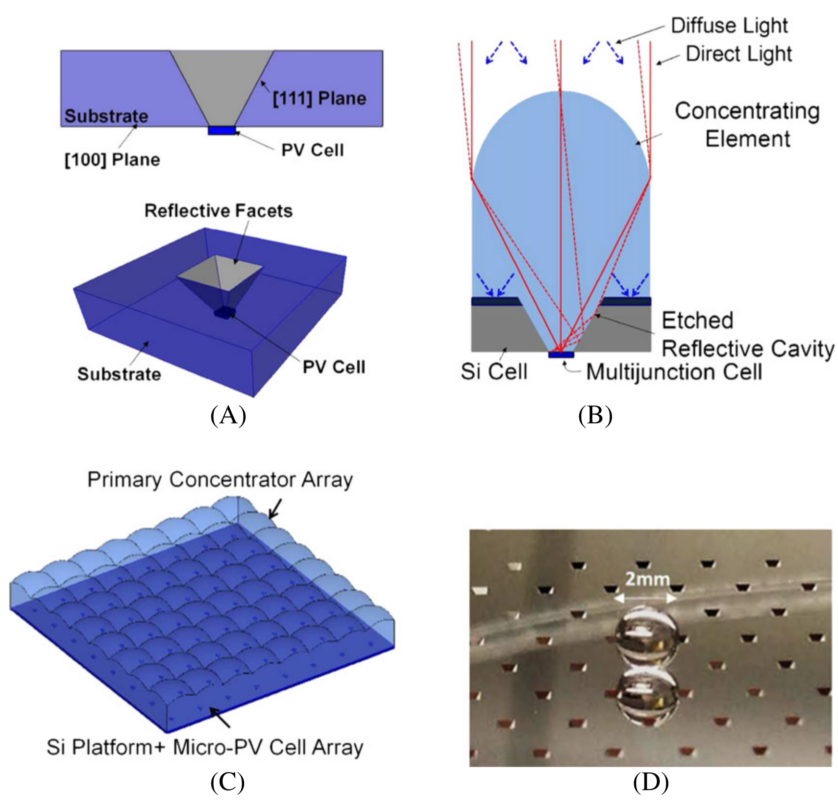

FIGURE 1 A, A novel multi-functional Si cell platform that integrates an array of concentrated multijunction micro-cells; B and C, a baseline structure consists of a molded lens array layer, a multi-functional Si cell, and an integrated array of high concentration multijunction micro-cells; D, self-aligned ball-lens concentrator on a Si cavity [Colour figure can be viewed at wileyonlinelibrary.com]

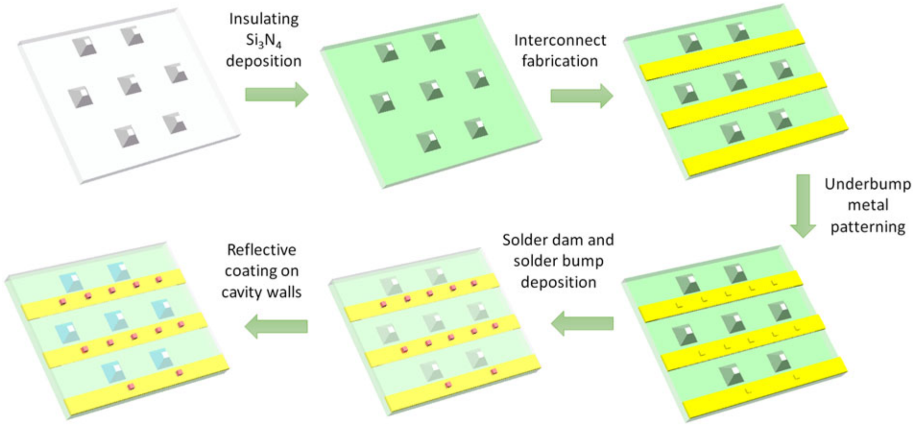

FIGURE 2 Schematic fabrication process flow for the multifunctional Si platform [Colour figure can be viewed at wileyonlinelibrary.com]

(thicknesses: 25 nm/100 nm/100 nm/200 nm, from bottom to top) underbump metal, sputtered silicon nitride (400-nm thickness) solder dam, and solder metal (5-μm SAC305, a lead-free alloy that contains 96.5% tin, 3% silver, and 0.5% copper) for the multijunction micro-cells were then sequentially patterned by contact photolithography and lift-off at the backside of the wafer. The interconnect and underbump metal layers were coated using electron beam evaporation whereas jet deposition was utilized to form the solder bumps. All these patterning steps were performed using dry film resist (Dupont MX 5020) to avoid the accumulation of resist in the etched cavities from the conventional spin coating technique. In the last step, the Si cavity sidewalls were coated with a 100-nm reflective silver metal film and a 150-nm silicon nitride protective layer to prevent oxidation of the metal coating. Multijunction micro-cells can then be solder bonded to the Si piece (not depicted in Figure 3). Figure 3A,B shows photos of the front and back sides of the fabricated Si platform.

The etched Si cavity sidewall quality was examined using white light interferometry. In the experiment, the etched Si wafers were cleaved along the [110] direction passing through the cavities, which divided the cavities in halves. The cleaved sample was then mounted onto a custom-made tilted sample holder such that one of the cavity's 4 sidewalls lies in the horizontal plane to facilitate the interferometry measurement. Figure 3C shows the exemplary surface morphology of the cavity sidewall characterized by white light interferometry. The measurement yields an average RMS roughness value of (10 ± 2) nm, introducing negligible scattering loss and thus minimum impact on the cavity's concentration performance when sunlight is incident on the sidewalls from the filling material (eg, PDMS).

Resistivity of the interconnect metal wires was measured to be 3.1×10^{-8} ohm·m, consistent with literature values of gold resistivity.[32] Based on the resistivity data, 2 interconnect designs were modeled to evaluate the ohmic power losses in micro-scale CPV modules. In a test module with 2 cm by 2 cm aperture, there are 11 rows of micro-cells, each containing 9 individual micro-cells arrayed in a honeycomb lattice pattern. In the first interconnect design, the micro-cells in each row are first stringed in series, and then all rows are connected in parallel. In the second layout, all cells are connected in parallel. Figure 4 compares the calculated fractional power loss from the test module due to ohmic resistance. While both design can achieve low power loss (< 2%) with a moderate gold film thickness of 300 nm, the series design claims much reduced power loss due to the smaller currents in the interconnect bus lines.

The results above indicate that the Si etched cavity platform fabricated using standard microfabrication protocols projects adequate optical and electrical performance for micro-cell array integration.

4 | OPTICAL PERFORMANCE CHARACTERIZATION

The etched Si cavity plays a critical role in simultaneously improving the concentration ratio and acceptance angle of a micro-CPV module with minimally added module complexity and costs. The optical performance of the Si platform is characterized by optically coupling the reflective cavity to an off-the-shelf N-BK7 ball lens concentrator, as shown in Figure 5A to C. The optical transmission of the ball lens

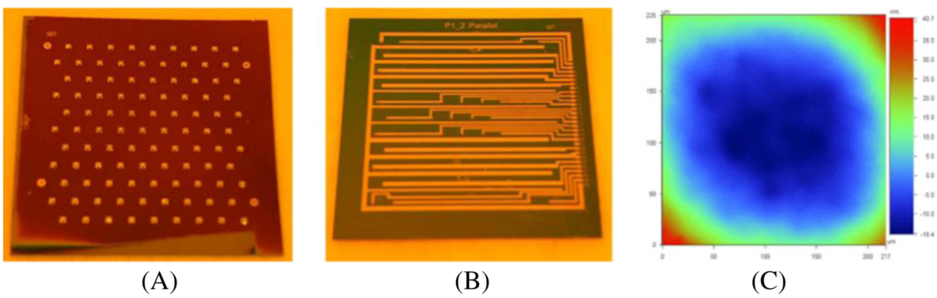

FIGURE 3 A, Frontside and B, backside photos of the Si platform with etched reflective cavities; the scale bar represents 5 mm; C, surface morphology of the Si cavity sidewall measured using white light interferometry [Colour figure can be viewed at wileyonlinelibrary.com]

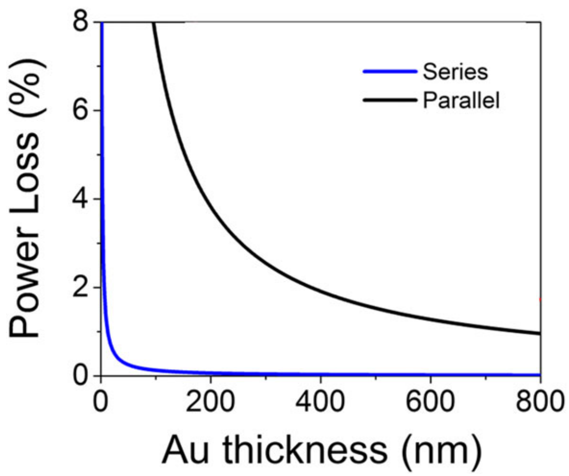

FIGURE 4 Simulated power loss due to ohmic resistance of interconnects: the 2 lines correspond 2 interconnect designs [Colour figure can be viewed at wileyonlinelibrary.com]

concentrator under different light incident angles is measured with and without integration with the Si reflective cavity attached to an off-the-shelf photodetector (PD). In order to emulate the micro-cell in the ball lens only measurement, an etched Si wafer is mounted reversely on the PD to act as a shadow mask that defines the 100 µm × 100 µm input optical aperture of the PD. The experimental setup is shown in Figure 5D. A fiber bundle light source is used to provide simulated direct normal sunlight with a divergence angle of approximately ±0.25°. The light source assembly are mounted on a custom-designed circular rail stage so that the beam's incident angle on the tested module can be precisely adjusted for angular response measurements. The ball lens and Si platform are mounted on linear-translation and tilt stages for alignment between the components.

The experimental results are shown in Figure 5E and compared with simulation results obtained from a ray-trace simulation model. At normal incidence, optical transmittances of 90.9% and 90.1% are measured for optical systems with and without the Si reflective cavity, respectively. The optical losses are primarily attributed to Fresnel losses at the non-AR-coated ball lens surface. Compared with simulation results, the experimental results indicate that the Si cavity enhances light collection by redirecting scattered light from the primary lens surfaces back to the cell region. The measured angular sensitivity further shows that acceptance angles (defined as the angular range with larger than 90% of on-axis power) of ±2.39° and ±1.14° are obtained for the optical systems with and without the Si cavity, respectively, indicating that the etched Si cavities significantly increase the angular tolerance of the baseline optical system.

The optical performance characterization results thus suggest that over 100% improvement on the concentration-acceptance-product is achieved by integrating the Si reflective cavity with a conventional optical concentrator. The mechanism for such *CAP* improvement can be explained by the increased incidence angle (with respect to the

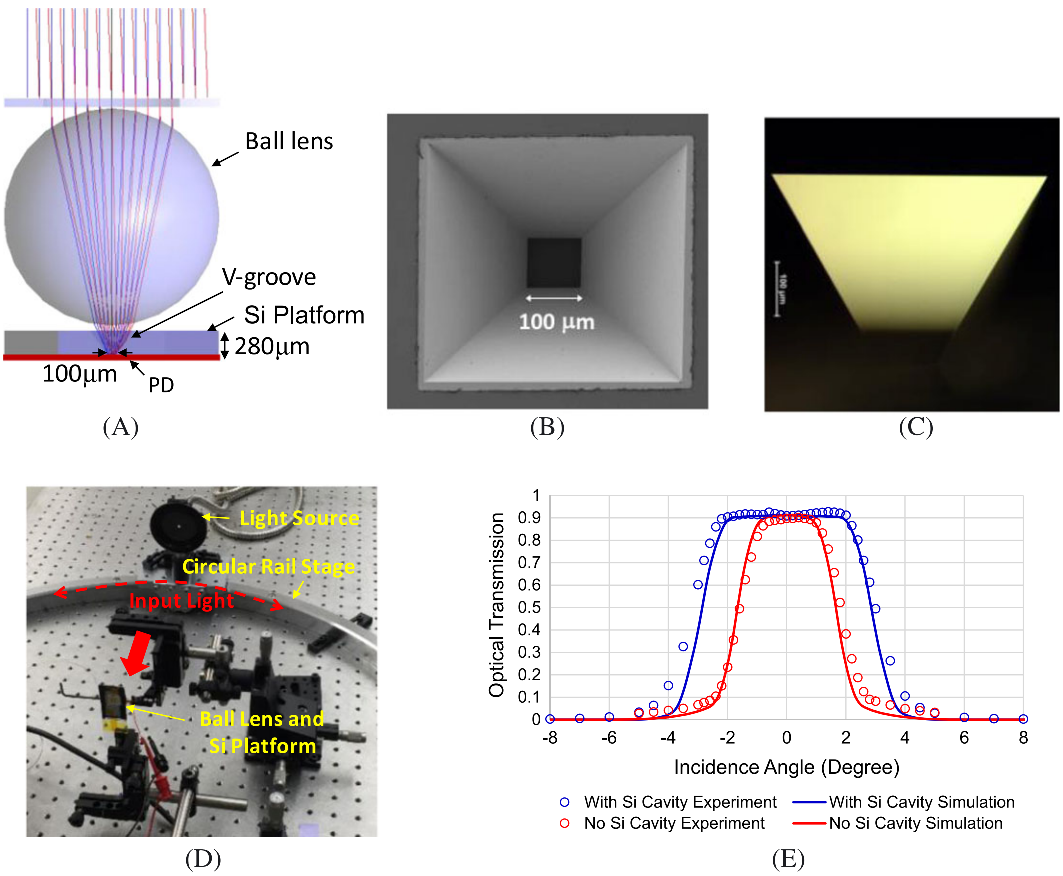

FIGURE 5 Optical performance characterization of etched Si cavity: A, optical simulation model; B, top view of an etched Si cavity after metallization; C, side view of an etched Si cavity; D, experiment setup; E, experimental vs simulation results indicate >100% improvement on acceptance angle and *CAP* by incorporating the low-profile Si cavity into a traditional optical concentrator system [Colour figure can be viewed at wileyonlinelibrary.com]

micro-cells) of light after reflection at the cavity sidewalls. The increased angular spread of incident light rays allows enhanced spatial confinement of incident light (ie, higher concentration ratio) according to the étendue conservation principle, leading to an improved *CAP* metric.

It should be noted that it is very challenging to accomplish such improvement cost-effectively by conventional optical concentrators due to the limited $f/\#$ of refractive elements and the significant fabrication challenges of making non-imaging elements at the micro-scale and in a large array format. On the contrary, the proposed WPV approach directly embeds such critical micro-optical elements in the wafer level, an approach suited for large-scale manufacturing.

5 | PROTOTYPE DEVELOPMENT

As schematically depicted in Figure 6A,B, the baseline prototypical module comprises a Si platform, an array of InGaP/GaAs micro-cells with 100-μm square apertures hybrid-integrated on the Si platform, a middle glass plate, and an aspheric PDMS primary lens array (~2.5-mm sub-lens diameter) directly molded on the glass. The micro-lenses, Si cavities, and micro-cells are arranged in hexagonal arrays to attain a 400× concentration ratio. The baseline structure is designed to have an acceptance angle of ±2.2°(> 90% of on-axis power), corresponding to a *CAP* of ~0.77, while the same optical system without the reflective Si cavities has an acceptance angle of ±1.2°according to our simulations. Furthermore, with a *CAP* of ~0.77 the baseline WPV design can be adapted to a 2000× concentration at a ±1° acceptance angle.

For component characterization and optimization purposes, our first prototype consists of 2 middle glass plates that hold the molded lens array and Si platform on their top and bottom surfaces, respectively. When assembled, they provide the same total effective optical path length as the design with a single middle glass plate. The primary PDMS lens array is molded on the glass, as shown in Figure 6C. The thickness of the optical system is less than 3 mm. The hybrid integration process of cells is demonstrated by flip-chip bonding micro-cell arrays to the interconnects on the Si platform via solder bumps. The resulting IIIV-on-Si platform is further bonded to a glass with PDMS as filler in the Si cavities. A test piece after the integration process is shown Figure 6D. The lens array was then aligned to the IIIV-on-Si cell platform. Both the lens array and integrated Si platform are packaged in Macor frames and the module is protected by a front cover glass. High-throughput, parallel micro-cell assembly approaches, such as transfer printing [20], can also be utilized for large-scale manufacturing.

The first-generation assembled prototype module was mounted on a 2-axis tracker (Figure 6E), and its acceptance angle was measured on-sun under a clear sky. Figure 6F shows the dependence of the output optical power on the incident angle of sunlight. Acceptance angles of ±1.7° and ±2.5° are measured for >90% of on-axis power and full-width-half-maximum, respectively. Compared with the simulation model (ie, black curve in Figure 6F), a gradual roll-off of the transmitted power is observed near the corners of the reflective cavity. This is due to particulates-induced air-bubbles accumulated on the cavity side-walls during the PDMS filling process, which can be eliminated in future generations. The measured full-width-half-maximum acceptance angle is in excellent agreement with the simulation model, thereby validating the performance improvement conferred by the Si platform.

6 | PERFORMANCE PROJECTION

The performance of the hybrid PV/CPV baseline design is projected by optical simulations under solar irradiation with a variety of direct/global irradiation ratios, representing different geological and weather scenarios.[33] The optical system is modeled and simulated using 3D non-sequential Monte Carlo ray-tracing under a combination of direct and diffuse light sources. The optical transmissions of the optical

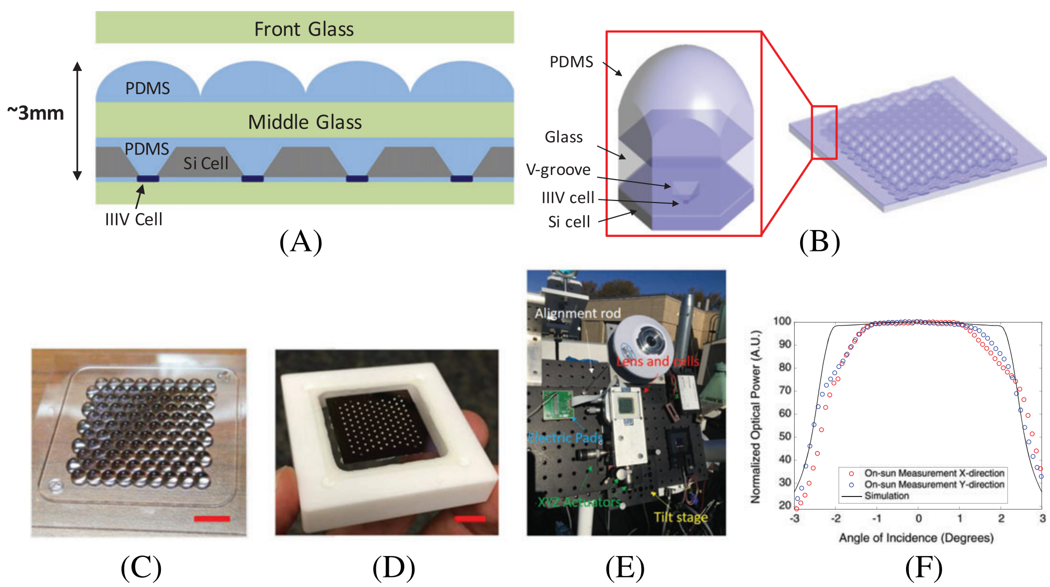

FIGURE 6 A, Schematic of baseline prototype module; B, baseline optical design; C, injection molded PDMS lens array on glass; D, hybrid integrated IIIV-on-Si platform bonded on glass and packaged in a Macor frame; the scale bar represents 5 mm; E, on-sun measurement setup: the assembled prototype module was mounted on a 2-axis tracker; F, acceptance angle measurement result vs simulation model [Colour figure can be viewed at wileyonlinelibrary.com]

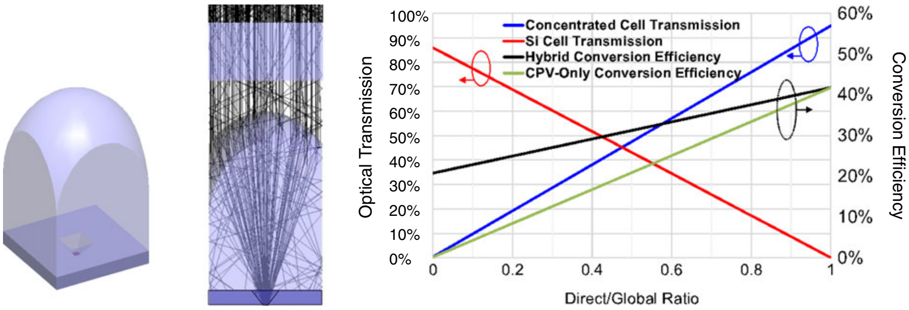

FIGURE 7 A, 3D Monte Carlo ray-tracing simulation model of a baseline design under simulated direct and diffuse light. B, Optical transmissions and conversion efficiency of the hybrid module vs Direct/Global Ratio. The simulation result of the hybrid module is compared with a CPV-only case of the same concentrator without the Si cell. Blue line: optical transmission on IIIV micro-cell; red line: optical transmission on Si cell; black line: calculated overall conversion efficiency combining contributions from both IIIV micro-cell and Si cell; green line: calculated conversion efficiency from the IIIV micro-cell only [Colour figure can be viewed at wileyonlinelibrary.com]

system onto the concentrated IIIV cell and the non-concentrated Si cell are plotted against the DNI/Global ratio, as shown in Figure 7. Assuming state-of-the-art 4-junction cells are used (~40% DNI module conversion efficiency), the overall conversion efficiency of the hybrid module is projected based on the optical simulation results and compared with a CPV-only case, also shown in Figure 7. It is clearly shown that between Direct/Global irradiation ratio of 0.75 to 0.6, the hybrid module provides a conversion efficiency improvement of 17% to 33% from the CPV-only case. In particular, the hybrid module is projected to achieve an efficiency over 30% for low DNI regions (ie, regions with ~60% DNI) that were typically considered not suitable for conventional CPV deployment.

7 | CONCLUSION

In summary, a novel micro-scale integrated PV/CPV concept is proposed and developed, which tightly integrates multijunction micro-cell and micro-optical concentrator arrays on a multi-functional Si platform. The Si platform simultaneously provides micro-optical concentration, hybrid photovoltaics, and micro-mechanical assembly functionalities. The wafer-embedded Si cavity concentrator is experimentally shown to provide over 100% improvement on the concentration-acceptance-angle product, leading to considerably reduced module costs, sufficient angular tolerance to low-cost trackers, and an ultra-compact flat-plate form factor. The development of a baseline prototype module and its optical performance characterization is described. The performance of the proposed approach under combined direct and diffuse irradiation is modeled and projected, indicating that the hybrid PV/CPV architecture can effectively extend the geographic and market domains for cost-effective PV system deployment. Leveraging low-cost micro-fabrication and high-level integration techniques, the micro-scale PV approach is capable of seamlessly combining the high performance of multijunction cells and the low costs of flat-plate Si PV systems.

ACKNOWLEDGEMENT

This work was supported by Advanced Research Projects Agency - Energy under the Micro-scale Optimized Solar-Cell Arrays with Integrated Concentration (MOSAIC) program (DE-AR0000632). The authors gratefully acknowledge Michael Haney, Eric Schiff, Zigurts Majumdar, James Zahler, Daniel Cunningham, and Gregory Nielson for their support, guidance and insightful discussions on this work.

Sandia National Laboratories is a multimission laboratory managed and operated by National Technology and Engineering Solutions of Sandia, LLC, a wholly owned subsidiary of Honeywell International, Inc., for the US Department of Energy's National Nuclear Security Administration under contract DE-NA0003525.

ORCID

Tian Gu http://orcid.org/0000-0003-3989-6927

REFERENCES

1. Fraunhofer ISE Photovoltaics Report, 2016.
2. Goodrich A, Hacke P, Wang Q, et al. A wafer-based monocrystalline silicon photovoltaics road map: utilizing known technology improvement opportunities for further reductions in manufacturing costs. *Sol Energy Mater Sol Cells*. 2013;114:110-135.
3. Maike Wiesenfarth DSK, Philipps SP, Bett AW, Horowitz K. Current status of concentrator photovoltaic (CPV) technology, 2017.
4. Luque A, Sala G, Luque-Heredia I. Photovoltaic concentration at the onset of its commercial deployment. *Prog Photovolt Res Appl*. 2006;14(5):413-428.
5. Swanson RM. The promise of concentrators. *Prog Photovolt Res Appl*. 2000;8(1):93-111.
6. Kurtz S, Myers D, McMahon WE, Geisz J, Steiner M. A comparison of theoretical efficiencies of multi-junction concentrator solar cells. *Prog Photovolt Res Appl*. 2008;16(6):537-546.
7. Benítez P, Mi ano JC, Zamora P, et al. High performance Fresnel-based photovoltaic concentrator. *Opt Express*. 2010;18(S1):A25.
8. Martin EDD, Green A, Emery K, Hishikawa Y, Warta W. Solar cell efficiency tables (version 47). *Prog Photovolt Res Appl*. 2015;24(1):3-11.
9. Steiner M, Siefer G, Schmidt T, Wiesenfarth M, Dimroth F, Bett AW. 43% sunlight to electricity conversion efficiency using CPV. *IEEE J Photovoltaics*. 2016;6(4):1020-1024.
10. Gu T, Li D, Li L, et al. Wafer-level integrated micro-concentrating photovoltaics. In *OSA Light, Energy and the Environment*, 2016.
11. Horowitz KAW, Woodhouse M, Lee H, Smestad GP. A bottom-up cost analysis of a high concentration PV module. *Cpv-11*. 2015;100001.
12. Gueymard CA. Fixed or tracking solar collectors ? Helping the decision process with the solar resource enhancement factor. *Proc SPIE*. 2008;7046:1-11.
13. Smestad G, Ries H, Winston R, Yablonovitch E. The thermodynamic limits of light concentrators. *Sol Energy Mater*. 1990;21(2–3):99-111.

14. Shatz N, Bortz J, Winston R. Thermodynamic efficiency of solar concentrators. *Opt Express*. 2010;18:A5-A16.
15. Miñano JC, Benítez P, Zamora P, Buljan M, Mohedano R, Santamaría A. Free-form optics for Fresnel-lens-based photovoltaic concentrators. *Opt Express*. 2013;21(Suppl 3, no. 103):A494-A502.
16. Gleckman P, O'Gallagher J, Winston R. Concentration of sunlight to solar-surface levels using non-imaging optics. *Nature*. 1989;339(6221):198-200.
17. Welford WT, Winston R. *High Collection Nonimaging Optics*. New York and London: Academic Press; 1989.
18. Gu T, Li D, Li L, et al. Wafer integrated micro-scale concentrating photovoltaics, *Photovolt. Spec. Conf. (PVSC), IEEE 44th*, 2017.
19. Haney MW. Can micro-CPV technology change the paradigm of flat-plate PV?. *Photovolt. Spec. Conf. (PVSC), IEEE 44th*, 2017.
20. Sheng X, Bower CA, Bonafede S, et al. Printing-based assembly of quadruple-junction four-terminal microscale solar cells and their use in high-efficiency modules. *Nat Mater*. 2014;13(6):593-598.
21. Lee K-T, Yao Y, He J, et al. Concentrator photovoltaic module architectures with capabilities for capture and conversion of full global solar radiation. *Proc Natl Acad Sci*. 2016;113(51):E8210-E8218.
22. Carlson A, Bowen AM, Huang Y, Nuzzo RG, Rogers JA. Transfer printing techniques for materials assembly and micro/nanodevice fabrication. *Adv Mater*. 2012;24(39):5284-5318.
23. Gu T, Agrawal G, Vessey A, et al. Micro-concentrator module for microsystems-enabled photovoltaics: optical performance characterization, modeling and analysis, in the proceeding of IEEE PVSC 2015. *Photovolt. Spec. Conf. (PVSC), 2015 IEEE 41st*, 2015.
24. Haney MW, Gu T, Agrawal G. Hybrid micro-scale CPV/PV architecture. *Photovolt. Spec. Conf. (PVSC)*, 2014 *IEEE 40th*, 2014:2122-2126.
25. Nielson GN, Okandan M, Cruz-Campa JL, et al. "Leveraging scale effects to create next-generation photovoltaic systems through micro- and nanotechnologies," 2012;8373(837317).
26. Ghosal K, Lilly D, Gabriel J, et al. Semprius field results and progress in system development. *IEEE J Photovoltaics*. 2014;4(2):703-708.
27. Jared BH, Saavedra MP, Anderson BJ, et al. Micro-concentrators for a microsystems-enabled photovoltaic system. *Opt Express*. 2014;22(S2): A521-A527.
28. Arase H, Matsushita A, Itou A, et al. A novel thin concentrator photovoltaic with microsolar cells directly attached to a lens array. *IEEE J. Photovoltaics*. 2014;4(2):709-712.
29. Lentine AL, Nielson GN, Okandan M, Cruz-Campa JL, Tauke-Pedretti A. Voltage matching and optimal cell compositions for microsystem-enabled photovoltaic modules. *IEEE J. Photovoltaics*. 2014;4(6):1593-1602.
30. Price JS, Sheng X, Meulblok BM, Rogers JA, Giebink NC. Wide-angle planar microtracking for quasi-static microcell concentrating photovoltaics. *Nat Commun*. 2015;6:6223.
31. Paap S, Gupta V, Tauke-Pedretti A, et al. Cost analysis of flat-plate concentrators employing microscale photovoltaic cells for high energy per unit area applications. In *Photovoltaic Specialist Conference (PVSC), IEEE 44th*, 2014:2926-2929.
32. Matula RA. Electrical resistivity of copper, gold, palladium, and silver. *J Phys Chem Ref Data Monogr*. 1979;8(4):1147-1298.
33. National Solar Radiation Database. [Online]. Available: https://nsrdb.nrel.gov/.

How to cite this article: Li D, Li L, Jared B, et al. Wafer integrated micro-scale concentrating photovoltaics. *Prog Photovolt Res Appl*. 2018;26:651–658. https://doi.org/10.1002/pip.3034